Volume 11, Number 5 (October 2018) p. 1076 – 1109 • ISSN 1983-4195
http://dx.doi.org/10.1590/S1983-41952018000500010

REVISTA IBRACON DE ESTRUTURAS E MATERIAIS
IBRACON STRUCTURES AND MATERIALS JOURNAL

Analysis of the effects of soil-structure interaction in reinforced concrete wall buildings on shallow foundation

Análise dos efeitos da interação solo-estrutura em edifícios de paredes de concreto sobre fundações superficiais

M. G. C. SANTOS [a]
marcell.gustavo@hotmail.com

M. R. S. CORRÊA [b]
marcio.correa@usp.br

Abstract

This paper presents a study of the effects caused by soil-structure interaction in reinforced concrete wall building on shallow foundation. It was verified the influence of displacements of supports on the redistribution of internal forces in the structural walls and in the redistribution of loads on the foundation. The superstructure was represented by shell finite elements and the soil-structure interaction was evaluated by iterative methods that consider the stiffness of the building, the soil heterogeneity and the group effect of foundation elements. An alternative model that considers the soil-structure interaction is adopted and the concrete walls are simulated by bar elements. The results indicate that the soil-structure interaction produces significant changes of the stress flow, with larger influences on the lower walls, as well as a tendency of settlements standardization and load migration to supports with smaller settlements.

Keywords: reinforced concrete wall building, structural analysis, shallow foundation, soil-structure interaction.

Resumo

Este artigo apresenta um estudo dos efeitos causados pela interação solo-estrutura em um edifício de paredes de concreto moldadas no local sobre fundações superficiais. Foi verificada a influência do deslocamento dos apoios na redistribuição dos esforços das paredes estruturais e dos carregamentos das fundações. A superestrutura foi discretizada em elementos finitos de casca e a interação solo-estrutura foi avaliada através de métodos iterativos, que consideram a rigidez da edificação, a heterogeneidade do solo e o efeito de grupo das fundações. Um modelo alternativo, em que a interação solo-estrutura é considerada de maneira simplificada e as paredes de concreto são discretizadas por elementos de barra, foi proposto e avaliado. Os resultados indicam que a interação solo-estrutura produz uma significativa modificação no fluxo de tensões, com maior influência nas paredes inferiores, bem como uma tendência de uniformização dos recalques e migração de carga para os apoios de menor recalque.

Palavras-chave: edifícios de paredes de concreto, análise estrutural, fundação superficial, interação solo-estrutura.

[a] *University of São Paulo, São Carlos School of Engineering, Department of Geotechnical Engineering, São Carlos, SP, Brazil;*
[b] *University of São Paulo, São Carlos School of Engineering, Department of Structural Engineering, São Carlos, SP, Brazil.*

Received: 12 Jul 2017 • Accepted: 05 Feb 2018 • Available Online: 28 Sep 2018

1. Introduction

A Concrete wall is a rationalized construction system that offers the advantages of high-scale production, in which the structure and the sealing are formed by a single system. In a concrete wall system, the window frames and electrical, sanitary and hydraulic installations can be incorporated. All the walls and slabs of the same cycle are concreted in a single step. Due to the high degree of industrialization, a concrete wall system is presented as a viable alternative. This constructive system is recommended for buildings that need to be executed quickly and that have a short delivery deadline and/or high repetition rate.

Behavior and structural analysis of reinforced concrete wall buildings has been topic of research in Brazil (Nunes [1] and Bragum [2]). The Brazilian National Standards Organization (NBR 16055:2012 [3]) regulates the quality, enforcement procedure and structural analysis of reinforced concrete wall buildings.

Traditionally, in the behavior analysis of reinforced concrete wall buildings, fixed supports are considered. However, the settlement of the foundation causes the internal force redistribution in the structural elements. In short, the reinforced concrete wall system behavior is governed by superstructure, infrastructure and soil interaction. This mechanism is called soil-structure interaction (SSI) and has been the topic of many studies (Meyerhof [4], Chamecki [5], Goshy [6] and Gusmão [7]). Testoni [8 and 9] and Santos [10] discussed SSI in reinforced concrete wall buildings.

Despite recent research and the design code, advances are still needed in knowledge regarding the reinforced concrete wall building behavior and their analysis models. In this paper, the procedures and results of an SSI analysis of a reinforced concrete wall building with 10 floors and a shallow foundation are presented.

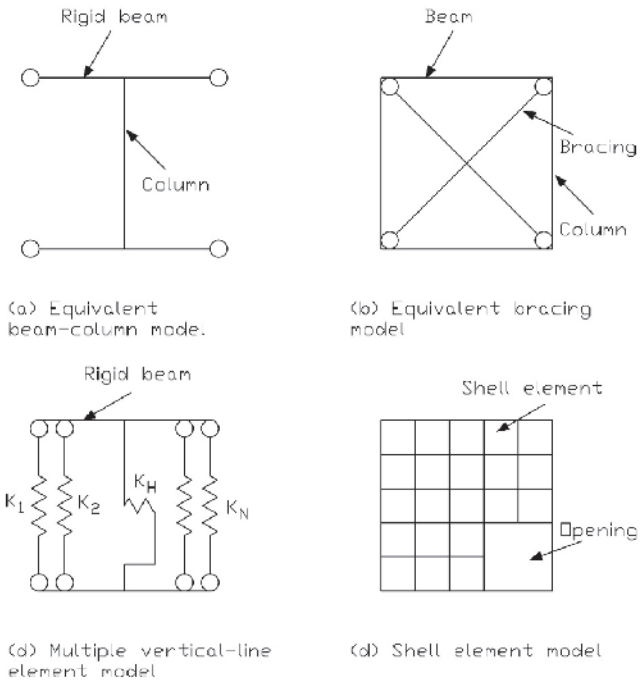

Figure 1
Modeling wall methods (Source: adapted from Liu *et al,* 2010)

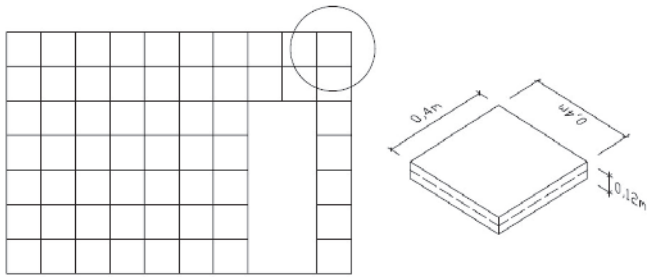

Figure 2
Discretization of the wall in shell elements

2. Numerical modeling of superstructure

The numerical analysis of structural walls can be carried out using discrete or continuous techniques. The discrete procedure enables more flexibility because it is able to solve problems with varied geometry and loads. Liu et al. [11] shows three general methods for the wall structural analysis following a discrete technique, as shown in Figure 1.

In this paper, two types of superstructure discretization were used. In the first one, called the SHELL model, discretization by shell elements was adopted, as shown in Figure 1d. This model provides accurate results that were not obtained using the beam elements, e.g. the internal force flow in the walls and consequent migration of the load for the supports. However, laborious computational modeling and result analysis can make it unfeasible for the daily use of structural design. Therefore, using a simplified model is preferred.

A second type of superstructure discretization, called MIXED model, to analyse a simplified model was considered. This model adopted equivalent beam-column elements (Figure 1a) above the second floor. Taking into account the effects caused by SSI, the shell elements on the two lower floors were kept. The finite element method (FEM) was used adopting the SAP2000 software to carry out the numerical analysis of the study building. The material was considered as linear elastic behavior.

To discretize the wall in the SHELL model, four-node quadrilateral shell finite elements (Shell-thin) were used with dimensions of 0.4mx0.4m and 0.12 thickness, as shown in Figure 2. Braguim [2] made comparisons between meshes with 0.2mx0.2m and 0.4mx0.4m dimensions and concluded that the differences in the results are practically non-existent. In this paper, a prior analysis was carried out to evaluate the influence of the mesh discretization on the results of the study building. The 0.4mx0.4m mesh element presents similar results to more refined mesh and a lower computational cost. The floor slab was considered as a rigid planar diaphragm.

In the MIXED model, the walls are discretized by frame elements. This discretization was based on Yagui [12 and 13], where the walls are replaced by the plane frame formed by horizontal rigid beams and a flexible column. This frames are join by a rigid floor

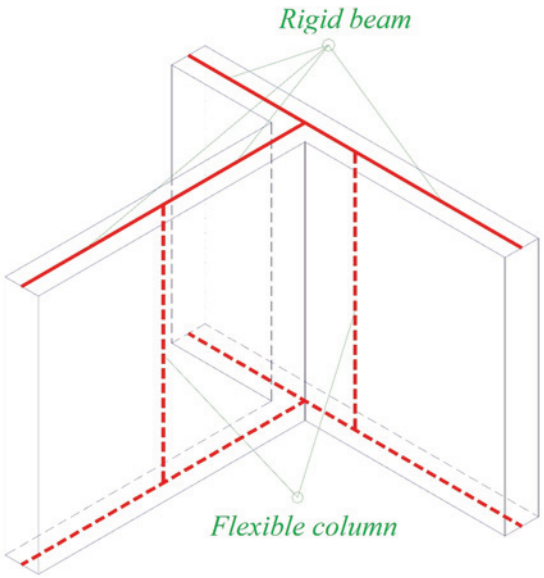

Figure 3
Discretization of the wall in frame elements (Source: Nascimento Neto, 1999)

slab (rigid planar diaphragm), forming a three-dimensional system. The columns must have the same geometric features as their respective walls and should be located in the geometric center of the walls. The walls are connected by a rigid horizontal beam and are applied on the floor level. Corrêa [14] recommends that the adopted value of beam rigidity is sufficiently large, as long as it does not disturb the numerical instability. In this paper, the Young's modulus value was multiplied by 100, as applied in Testoni [8]. Figure 3 shows a schematic drawing of the equivalent beam-column element discretization. The connection between two rigid beams are considered joints, where the only vertical shear stress is only taken into account. In this model, door and window openings are considered as flexible beams of infinite axial rigidity as shown in Figure 4.

According to NBR 16055:2012 [3], the wall of the structural system can be represented by a linear element as long as the shear deformation is considered. Nascimento Neto [15] suggests a refinement of the model proposed by Yagui [12 and 13] to consider shear deformation in a simplified way. A shape factor of c = 1.2 was used to reduce the section area of the walls and determine the equivalent shear area ($A_s = A_c/c$).

In the three-dimensional frame model proposed by Yagui [12 and 13] it is not possible to analyse the migration tendency of the load for the supports. Considering this behavior on the structural model, the walls of the first and second floor had to be discretized by shell elements, based on Nunes [1] and Testoni [8 and 9]. In this model, the first and second floors were discretized by a 0.2mx0.2m mesh to ensure that all the columns were connected to a node of the shell element.

3. Methodology for SSI analysis

Aoki [6] proposed an iterative procedure based on Chamecki [5] for the SSI analysis. This methodology analysed the separate superstructure of the foundation, searching for a final balance configuration through the displacement compatibility of the superstructure/foundation.

Initially, the support loads considering the rigid base hypothesis are calculated. These loads are used to calculate the shallow foundations. The shallow foundation are considered rigid elements and a linear pressure diagram is allowed at the base/soil contact.

The Mindlin [17] equations calculate the strain and stress in the soil points caused by a normal force. These equations consider the soil as an elastic isotropic and semi-infinite solid. Figure 5 presents the variables involved in this problem. The displacements of the shallow foundations are calculated by Eq. (1).

$$r_z = \frac{P(1+\nu)}{8\pi E(1-\nu)}\left[\frac{3-4\nu}{R_1} + \frac{8(1-\nu)^2-(3-4\nu)}{R_2} + \frac{(z-c)^2}{R_1^3} + \frac{(3-4\nu)(z+c)^2-2cz}{R_2^3} + \frac{6cz(z+c)^2}{R_2^5}\right] \quad (1)$$

Where P is the normal force, c is the depth of applying the normal force, v is the PoSSIon's ratio, B (x,y,z) is the point where the displacements are determined, z is the depth of the B (x,y,z) point and E is the Young's modulus. R_1 and R_2 are calculated by the geometric properties.

In order to determine the displacements, the base of the loaded footing in subareas was discretized in which the occurrence of a

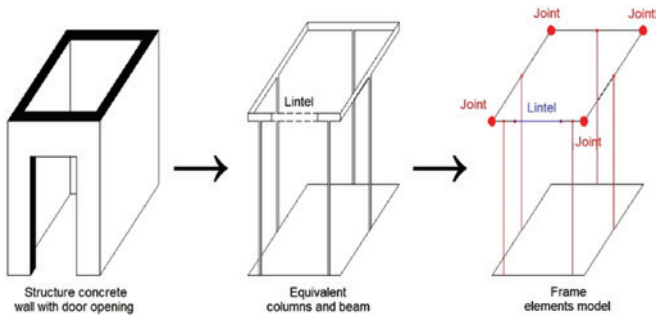

Figure 4
Representation of the lintels

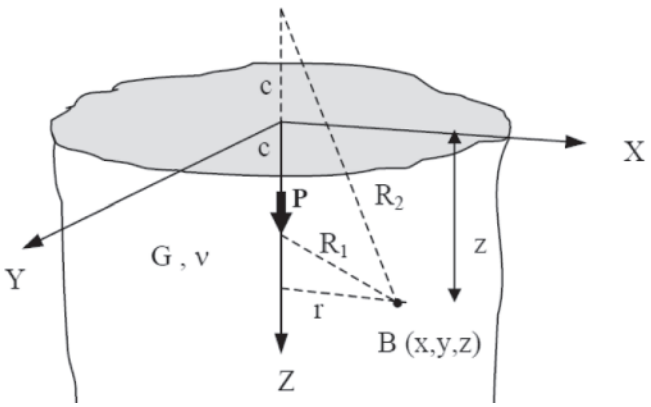

Figure 5
Semi-infinite elastic medium (Source: Mindlin, 1936)

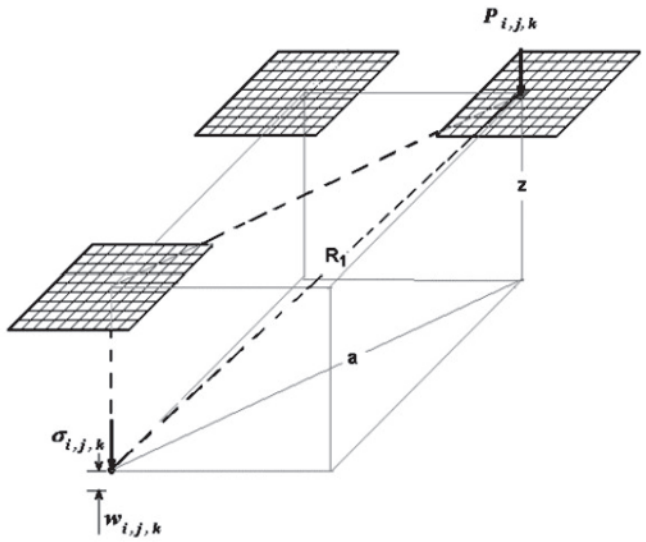

Figure 6
SSI model (Source: Reis, 2000)

concentrated load can be considered. In order to consider the group effect, the settlements are added due to the loads of all the footings in the building, according to Figure 6.

The total settlement δ of footing k is calculated in the geometric centre of its base by Eq. (2). The rotations in the footings were determined directly by the settlements obtained at their ends, according to Figure 7. The stratification of the soil mass is considered using Steinbrenner's technique [18].

$$\delta_k = \sum_{k=1}^{n^o\ of\ footings} \sum_{i=1}^{n_1} \sum_{j=1}^{n_2} r_{z_{ijk}} \quad (2)$$

After determining the vertical settlements and the footing rotations, the spring coefficients are determined by dividing the reactions of each support by the corresponding displacements. The calculated spring coefficients are imposed on the superstructure supports. Then the superstructure is recalculated and the new support reactions are determined. The whole procedure is repeated until the values of the reactions converge or the settlements are obtained between two consecutive iterations within a desired tolerance. More details about the methodology adopted can be found in Santos [10]. In this paper, the convergence criterion presented in Eq. (3) was applied, with tolerance $\xi = 10^{-3}$.

$$\sum_{k=1}^{n^o\ of\ footings} \frac{\|P_k - P_k^*\|^2}{\|P_k\|^2} \leq \xi \quad (3)$$

Where P_k is the axial force of footing k in the current iteration, P_k^* is the axial force of footing k in the previous iteration and ξ is the tolerance.

A computational routine was developed in MATLAB v7.10.0. to automate this procedure.

4. Building description

The evaluated building is the same one adopted in Braguim´s study [2] and is an adaptation of the *Condomínio das Árbores* building, built in the city of *São Bernado do Campo*, Brazil designed by the company *OSMB Engenheiros Associados Ltda*. The adapted building has ten floors, wall thicknesses of 0.12m, slab thicknesses of 0.10m and ceiling of 2.80m.

The adaptations aimed to simplify the computational modelling and basically consisted of considering all floors equal to the type and modifying all measurements for multiples of 0.4m. The layout and names of the walls are shown in Figure 8. The abbreviations PH and PV were used for the horizontal and vertical walls, respectively. The wall lengths are shown in Table 1.

Reinforced concrete was considered as isotropic material with the

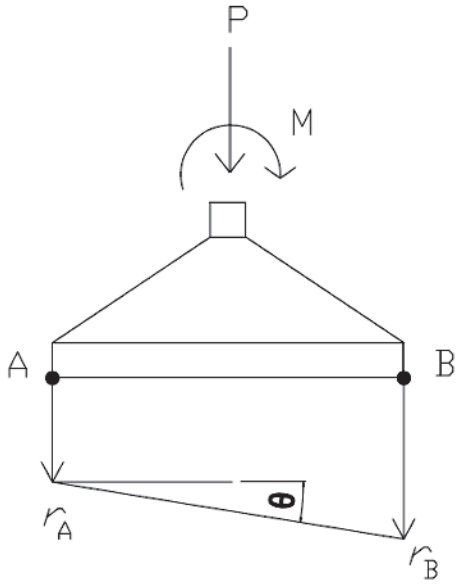

Figure 7
Determination of rotation in the shallow foundation

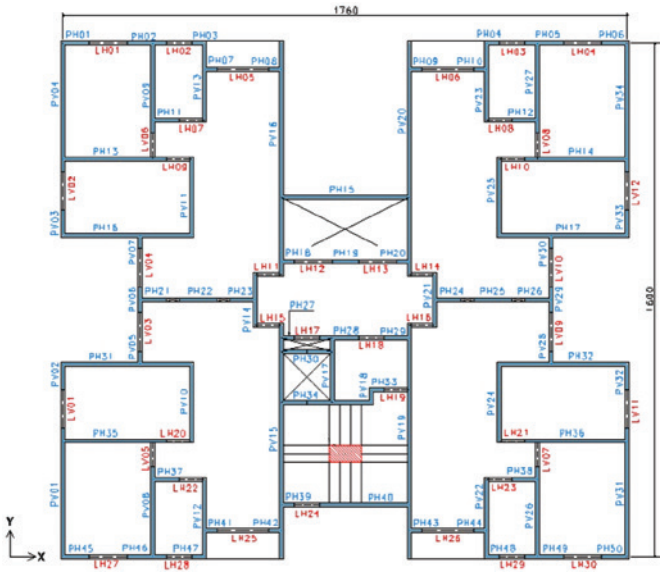

Figure 8
Floor plan of the building (Source: Braguim, 2013)

Table 1
Length of walls

Wall	Length (m)
PH03, PH04, PH07, PH08, PH09, PH10, PH18, PH20, PH27, PH33, PH39, PH41, PH42, PH43, PH44, PH47, PH48, PV05, PV07, PV18, PV28 and PV30	0.40
PH01, PH06, PH11, PH12, PH19, PH21, PH23, PH24, PH26, PH29, PH37, PH38, PH45, PH50, PV02, PV03, PV06, PV29 PV32 and PV33	0.80
PH02, PH05, PH22, PH25, PH28 PH46 and PH49	1.20
PH30, PV14 and PV21	1.60
PV17	2.00
PV10, PV11, PV12, PV13, PV22, PV23, PV24 and PV25	2.40
PH34, PH40, PV08, PV09, PV26 and PV27	2.80
PH13, PH14, PH35 and PH36	3.20
PH15, PH16, PH17, PH31, PH32, PV01, PV04, PV31 and PV35	4.00
PV15, PV16, PV19 and PV20	7.2

following mechanical properties: compression strength of 25MPa, secant modulus of elasticity of 24GPa, PoSSIon coefficient of 0.2 and specific weight of 25kN/m³. In the analysis, only vertical loads were considered: dead load (sum of the weight of the structure with the slab coating loads) and live loads (overhead of residential building slabs according to NBR 6120: 1980 [20]). The stairs were simplified by considering a slab with a thickness of 0.12m. The load distribution of the slabs on the walls was done adopting the yield line theory, using the values presented in Table 2.

A ground beam was considered under the building with cross section dimensions of 0.2mx0.5m. In the computational model, the ground beam was discretized by beam elements. A total of 47 shallow foundation were used at 1.5m depth, according to Figure 9. The foundation design was defined after considering the

Table 2
Slab loads

Dead load for h=10cm	Dead load for h=12cm	Live load for h=10cm	Live load for h=12cm
3.5 kN/m²	4.0 kN/m²	1.5 kN/m²	2.5 kN/m²

Table 3
Characteristics of the footings

Found.	SPT	A (m)	B (m)	H (m)	Found.	SPT	A (m)	B (m)	H (m)
F01	S1	2.0	2.0	0.8	F24	S2	2.3	1.8	0.8
F02	S1	1.8	2.5	0.9	F25	S3	1.9	1.5	0.6
F03	S2	1.8	2.5	0.9	F26	S2	1.9	1.5	0.6
F04	S2	2.0	2.0	0.8	F27	S1	2.0	2.0	0.8
F05	S1	2.2	2.2	0.8	F28	S3	2.0	2.0	0.8
F06	S2	2.2	2.2	0.8	F29	S2	2.0	2.0	0.8
F07	S1	1.2	2.7	0.9	F30	S2	2.0	2.0	0.8
F08	S1	1.9	0.8	0.8	F31	S3	3.5	1.9	1.1
F09	S2	1.9	0.8	0.8	F32	S3	3.5	1.8	1.1
F10	S2	1.2	2.7	0.9	F33	S3	2.5	2.5	0.9
F11	S1	2.5	2.5	0.9	F34	S3	1.1	1.5	0.6
F12	S1	1.1	1.5	0.6	F35	S3	1.1	1.5	0.6
F13	S2	1.1	1.5	0.6	F36	S2	2.5	2.5	0.9
F14	S2	2.5	2.5	0.9	F37	S3	3.5	1.2	1.1
F15	S1	3.0	2.0	1.0	F38	S3	1.2	2.7	0.9
F16	S2	3.0	2.0	1.0	F39	S3	1.9	0.8	0.8
F17	S1	2.0	2.0	0.8	F40	S3	1.9	0.8	0.8
F18	S1	2.0	2.0	0.8	F41	S3	1.2	2.7	0.9
F19	S2	2.0	2.0	0.8	F42	S3	2.2	2.2	0.8
F20	S2	2.0	2.0	0.8	F43	S3	2.2	2.2	0.8
F21	S1	1.9	1.5	0.6	F44	S3	2.0	2.0	0.8
F22	S2	1.9	1.5	0.6	F45	S3	1.8	2.5	0.9
F23	S1	2.3	1.8	0.8	F46	S3	1.8	2.5	0.9
–	–	–	–	–	F47	S3	20	2.0	0.8

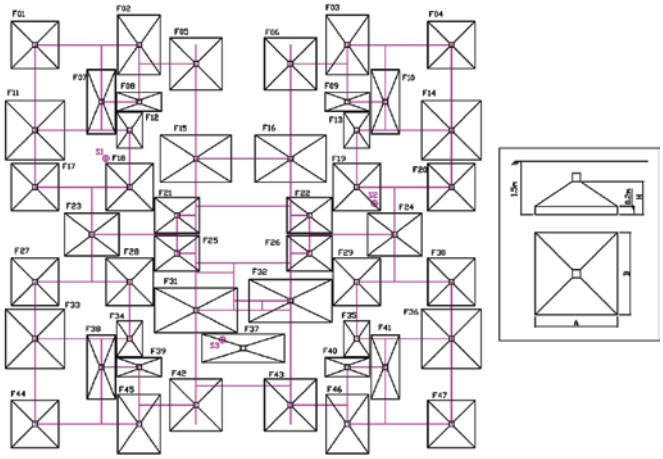

Figure 9
Foundation plan

normal loading results of the model with fixed supports, assuming the symmetry of the foundations. Table 3 shows the characteristics of the shallow foundations adopted in the design.
To characterize the soil type, the boreholes used in Santos' paper were adopted [10]. This profile has three SPT (Standard Penetration Test) boreholes, identified by S1, S2 and S3, located according to the Figure 9. Table 4 presents a summary of the Young's modulus values for each soil layer considered in the borehole. The PoSSIon coefficient was adopted at 0.30 for all layers. The Young's modulus values were estimated based on the soil parameters, as described in Santos [10].

5. Results and discussion

In the first series of comparisons, the effects produced in the building after considering the soil-structure interaction are presented. To do this, comparisons are made between the SHELL model with the rigid supports (SHELL RIG) and the SHELL model with the movable supports (SHELL SSI), using the methodology described in item 3. The results of the normal stress in the walls, the loads applied to the foundations and the settlements of the shallow foundations are presented. The desired convergence in the sixth iteration was obtained using the SHELL SSI model.
In the second series of comparisons, the results of the proposed simplified model (MIXED model) are presented. The results obtained in the MIXED model are compared with the reference model (SHELL model). In the simplified model analysis, the soil-structure interaction is addressed in two ways. In the first one, called the MIXED SSI model, the soil-structure interaction is considered using the methodology presented in item 3. In the second approach, called the MIXED SIMP model, the spring coefficients are determined by the estimated settling method, which basically consists of dividing the reactions of each support by its settlement, obtained by Mindlin's equation [17]. In practice, the spring coefficient of the MIXED SIMP model is determined in the first iteration, while the spring coefficient for the MIXED SSI model is obtained after convergence of the algorithm, according to the criterion presented in Eq. (3). The MIXED SSI model produced the desired convergence in the seventh iteration.
According to NBR 8681 [21], the weighting coefficient γ_f can be considered as the product of two others, γ_{f1} and γ_{f3}. The partial coefficient γ_{f1} considers the variability of actions and coefficient γ_{f3} considers the possible errors of evaluation of the effects of the actions, either by constructive problems or by deficiency of the calculation methods. Therefore, considering the weighting coefficient γ_f =1,4 for the normal considerations, the γ_{f1} and γ_{f3} coefficients can unfold in the product of two equal values, i.e., $\gamma_{f1} = \gamma_{f3}$= 1.18. Thus, the variation of 18% would be considered covered by γ_{f3} = 1.18.
In this paper, the differences below 5% are considered as an excellent approximation. Values between 5 and 18% are considered good or satisfactory approximation. Differences above 18% are considered bad or unacceptable.

5.1 First series of comparisons

Initially, the effects caused by considering the soil-structure interaction in the normal stresses of the building´s walls were evaluated. The normal stresses (at the foundation level) of the building´s walls are presented and compared in Table 5.
Consideration of the soil-structure interaction generated a redistribution of the stresses of the building walls, with a mean absolute deviation of 34%. This redistribution of stresses is accounted for by the high rigidity of the superstructure, which limits differential settlements and sets a trend towards settlement uniformisation. Therefore, symmetrical walls with the same geometric characteristics present different normal stresses due to soil heterogeneity.
Among all the walls of the building, 64% presented differences greater than 18% and out of these, approximately half had an increase of normal requests. There are marked increases in stresses, for example on PH04, PH43, PH44 and PH50 walls which increased by more than 100% and which would exceed the normalized resistance limits.
Figure 10 shows the normal force diagrams on some of the building´s walls. We decided to analyse PH01, PH02, PH03, PH13, PH15, PV06, PV09, PV13 and PV16 walls because they had different characteristics (length, door and window openings, etc.) and

Table 4
Young's modulus values

Borehole (SPT)	Depth (m)		E (MPa)
	Start	End	
S1	0.00	1.50	12.60
	1.50	3.00	32.40
	3.00	7.00	142.40
	7.00	10.00	292.80
S2	0.00	3.00	11.20
	3.00	4.00	21.12
	4.00	6.00	136.40
	6.00	10.00	194.70
S3	0.00	1.50	11.88
	1.50	3.00	28.36
	3.00	7.00	90.44
	7.00	10.00	194.40

are subject to different levels of loading. The percentage values in the graph indicate the differences in normal forces between the SHELL RIG and SHELL SSI models.

It can be observed that the greatest differences between the normal stress values in the building´s walls occur, as expected, on the lower floors. However, in some of the building´s walls, the influence of the soil-structure interaction affected the upper floors, for example in the PH03, PV13 and PV16 walls.

The loads applied in the building´s foundation obtained from the shell model with the fixed supports were compared with the loads obtained from the shell model on the flexible supports, presented in Table 6. Figure 11 shows a graph of the dispersion of values of the vertical load applied in the foundations. In this graph, the peripheral foundations are highlighted by vertical lines.

Table 5
Normal wall force – kN

Wall	Shell RIG	Shell SSI	Differ. (%)	Wall	Shell RIG	Shell SSI	Differ. (%)
PH01	199.6	268.9	35	PH45	194.9	193.9	0
PH02	23.3	26.2	12	PH46	23.3	15.9	-32
PH03	127.5	243.2	91	PH47	126.5	191.4	51
PH04	124.4	268.0	115	PH48	123.1	237.9	93
PH05	24.4	18.7	-24	PH49	24.7	35.6	44
PH06	205.1	283.6	38	PH50	199.8	431.0	116
PH07	37.2	52.0	40	Column	630.0	630.0	0
PH08	122.8	209.1	70	PV01	657.1	493.0	-25
PH09	126.3	50.5	-60	PV02	199.6	194.2	-3
PH10	35.0	52.0	49	PV03	197.3	194.8	-1
PH11	212.0	174.7	-18	PV04	658.1	716.4	9
PH12	208.9	123.4	-41	PV05	11.5	12.3	7
PH13	358.8	399.9	11	PV06	233.6	227.4	-3
PH14	362.8	257.5	-29	PV07	11.1	7.4	-33
PH15	560.2	498.9	-11	PV08	404.1	300.3	-26
PH16	538.6	625.6	16	PV09	396.1	370.7	-6
PH17	539.9	469.1	-13	PV10	505.0	369.8	-27
PH18	-14.9	-17.7	19	PV11	508.0	548.1	8
PH19	24.0	18.0	-25	PV12	479.7	458.6	-4
PH20	-15.7	-6.5	-59	PV13	469.6	575.1	22
PH21	73.0	129.0	77	PV14	495.3	594.4	20
PH22	214.9	214.9	0	PV15	1464.1	1131.7	-23
PH23	-53.2	-36.5	-31	PV16	1069.7	1689.0	58
PH24	-49.7	-76.7	54	PV17	21.6	13.7	-37
PH25	214.9	214.9	0	PV18	19.0	21.4	13
PH26	68.0	129.0	90	PV19	1383.2	1320.0	-5
PH27	20.3	25.0	23	PV20	1093.4	777.8	-29
PH28	24.0	28.5	19	PV21	490.7	391.0	-20
PH29	12.9	3.4	-74	PV22	471.2	580.6	23
PH30	38.1	28.2	-26	PV23	460.4	364.7	-21
PH31	545.6	604.1	11	PV24	487.4	445.8	-9
PH32	547.1	401.0	-27	PV25	490.9	337.5	-31
PH33	84.9	106.0	25	PV26	406.3	503.5	24
PH34	412.7	310.5	-25	PV27	397.4	271.7	-32
PH35	362.1	354.1	-2	PV28	11.5	3.4	-70
PH36	366.1	259.0	-29	PV29	235.2	218.7	-7
PH37	216.7	134.7	-38	PV30	11.0	7.9	-28
PH38	213.4	217.8	2	PV31	679.4	973.0	43
PH39	33.0	27.9	-15	PV32	209.9	233.8	11
PH40	110.3	97.8	-11	PV33	207.7	237.3	14
PH41	35.4	33.6	-5	PV34	680.1	713.0	5
PH42	170.4	126.5	-26	SUM	24509.3	24960.8	–
PH43	177.4	425.0	140	Average	–	–	34
PH44	32.8	154.2	371	–	–	–	–

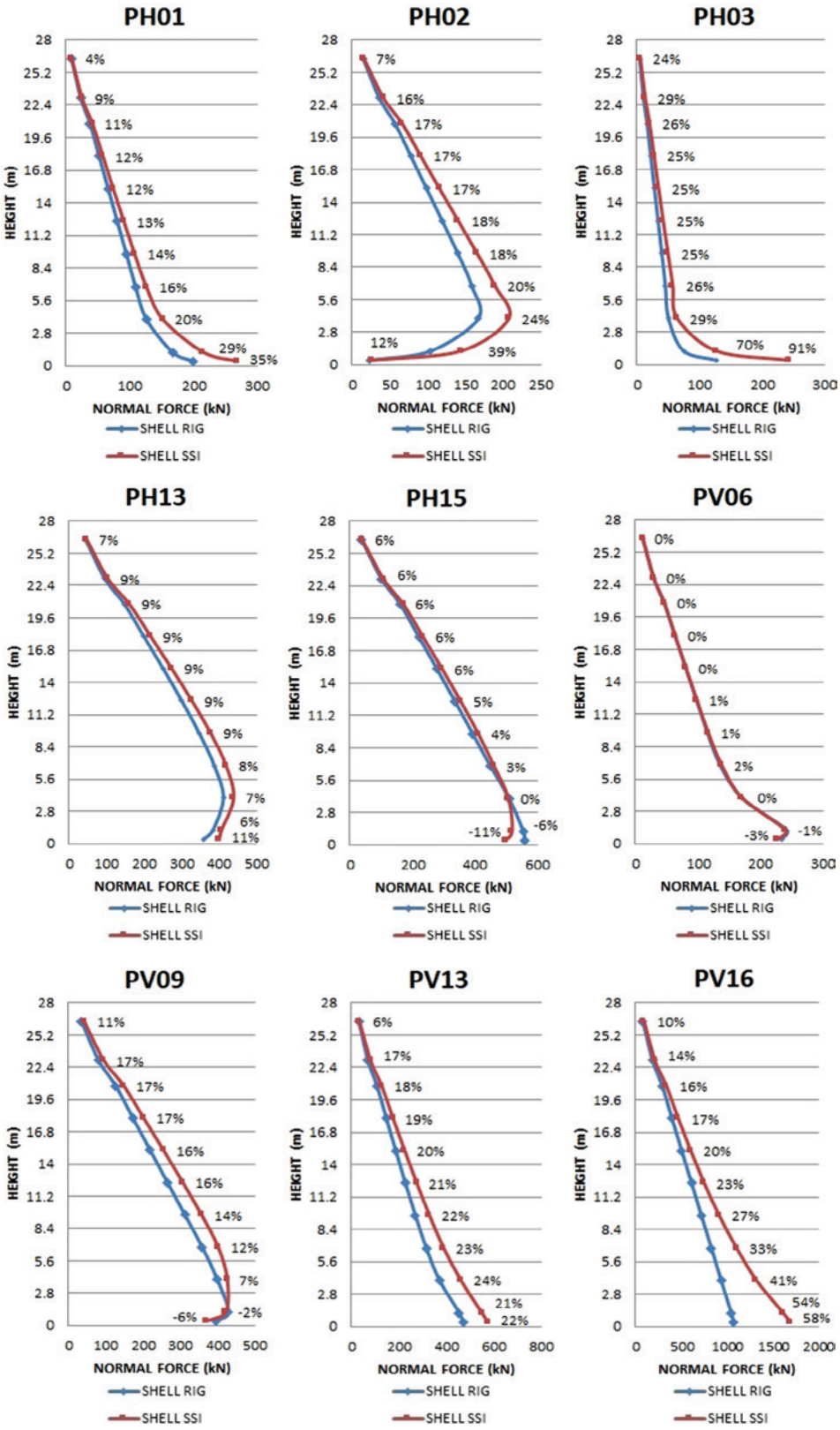

Figure 10
Normal force diagram of the buildings walls

Table 6
Loading of the foundations – kN and kN.m

Found.	Nz			Mx			My		
	Shell RIG	Shell SSI	Differ. (%)	Shell RIG	Shell SSI	Differ. (%)	Shell RIG	Shell SSI	Differ. (%)
F01	508.9	701.7	38	-47.7	-67.4	41	-46.6	-83.4	79
F02	521.9	791.6	52	-45.3	23.1	-151	49.2	1.5	-97
F03	509.8	535.7	5	-44.2	0.0	-100	-48.8	-12.9	-74
F04	526.8	628.7	19	-49.4	21.3	-143	47.5	5.6	-88
F05	582.6	1073.8	84	-9.5	0.0	-100	26.1	0.0	-100
F06	590.7	470.2	-20	-9.8	0.0	-100	-26.7	8.5	-132
F07	584.7	519.0	-11	10.7	0.0	-100	-29.0	0.0	-100
F08	290.4	262.6	-10	42.6	0.0	-100	17.6	0.0	-100
F09	283.0	179.3	-37	41.7	0.0	-100	-16.9	0.0	-100
F10	583.6	375.2	-36	11.8	0.0	-100	27.8	0.0	-100
F11	747.6	805.0	8	12.6	0.0	-100	-51.8	-138.9	168
F12	331.2	278.5	-16	-45.2	0.0	-100	41.7	0.0	-100
F13	319.3	184.4	-42	-43.8	0.0	-100	-39.6	-1.0	-97
F14	772.9	719.3	-7	12.8	0.0	-100	52.0	0.0	-100
F15	872.4	1196.5	37	-2.9	0.0	-100	-53.4	-55.3	4
F16	900.2	505.8	-44	-3.1	0.0	-100	54.1	-15.9	-129
F17	470.8	545.1	16	35.2	-4.6	-113	-47.4	-106.0	123
F18	541.6	580.2	7	44.7	41.4	-7	50.0	0.0	-100
F19	519.0	388.2	-25	43.0	7.8	-82	-49.0	-17.1	-65
F20	495.1	501.0	1	37.0	0.0	-100	48.7	0.0	-100
F21	347.3	520.5	50	-41.9	-31.9	-24	-44.8	-36.6	-18
F22	346.3	256.5	-26	-41.4	0.0	-100	44.8	0.0	-100
F23	592.0	637.4	8	0.0	0.0	0	-72.6	-109.8	51
F24	591.7	440.7	-26	1.0	7.2	616	71.7	1.9	-97
F25	384.7	328.9	-15	40.3	0.0	-100	-70.7	-52.9	-25
F26	359.1	186.8	-48	40.8	0.0	-100	55.2	0.0	-100
F27	478.1	572.4	20	-35.6	70.7	-299	-48.1	-113.8	137
F28	548.3	406.8	-26	-44.8	-9.1	-80	50.6	0.0	-100
F29	525.9	267.2	-49	-43.1	0.0	-100	-49.6	0.0	-100
F30	503.4	488.0	-3	-37.4	0.0	-100	49.4	0.0	-100
F31	1337.1	887.1	-34	10.3	0.0	-100	-87.0	-111.8	29
F32	906.7	1134.7	25	0.0	0.0	0	69.8	31.9	-54
F33	755.1	593.9	-21	-12.2	0.0	-100	-52.3	-186.5	256
F34	325.4	194.7	-40	44.6	0.0	-100	42.2	0.0	-100
F35	312.0	377.3	21	43.0	0.0	-100	-39.9	-24.6	-39
F36	782.1	586.8	-25	-12.3	0.0	-100	52.5	0.0	-100
F37	630.0	630.0	0	1.0	0.0	-100	-7.1	-138.8	1867
F38	597.2	411.2	-31	-10.2	0.0	-100	-29.6	0.0	-100
F39	301.4	210.0	-30	-43.9	0.0	-100	17.9	-3.4	-119
F40	295.1	264.8	-10	-43.1	0.0	-100	-17.2	3.0	-117
F41	597.7	718.0	20	-11.2	17.5	-257	28.4	0.0	-100
F42	824.7	741.0	-10	22.3	0.0	-100	32.7	0.0	-100
F43	857.0	934.7	9	25.2	0.0	-100	-34.4	-574.5	1571
F44	496.9	542.2	9	47.1	81.0	72	-45.6	-74.4	63
F45	519.6	637.3	23	45.8	-6.6	-114	48.5	0.0	-100
F46	505.5	815.4	61	44.7	-7.5	-117	-48.0	-53.6	12
F47	513.2	1159.8	126	48.8	133.9	174	46.3	34.5	-25
Total	26185.8	26185.8	–	–	–	–	–	–	–
Average	–	–	27	–	–	113	–	–	160

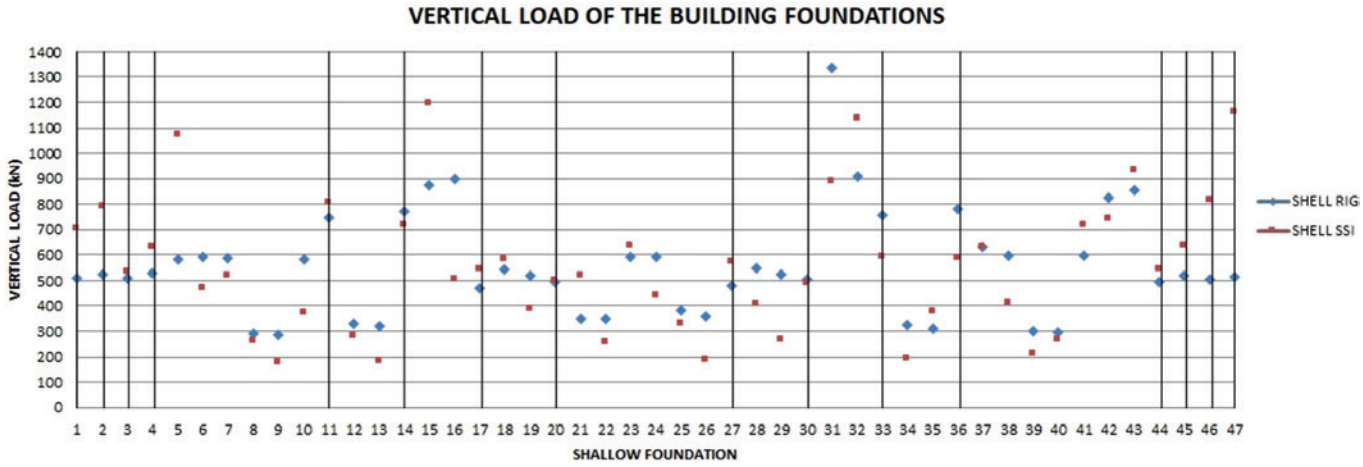

Figure 11
Scatter plot of the vertical load of the building foundations

In general, load redistribution occurred in the building´s foundations with a mean absolute deviation of 27%. Approximately 64% of the foundations showed differences of more than 18%, highlighting the increase of 126% in the F47 footing. There was also a tendency to reduce the bending moment in both directions, where the majority of the values were cancelled.

The mechanism that governs the load redistribution in the supports is the tendency to standardize the settlements. In the analysed building, the foundations located in the region of the S2 borehole show the behaviour of yielding to the neighborhood, since this region presented the highest settlements. There is also a trend of load transfer to the peripheral foundations.

Table 7 shows the vertical displacement of the supports of the building and Table 8 presents some information about the behaviour of the

Table 7
Settlement of the building supports – mm

Found.	Shell RIG	Shell SSI	Differ. (%)	Found.	Shell RIG	Shell SSI	Differ. (%)
F01	3.2	4.3	35	F24	12.5	9.3	-25
F02	3.6	5.4	47	F25	6.6	6.0	-9
F03	9.7	9.5	-2	F26	12.5	8.5	-32
F04	9.1	10.7	18	F27	3.8	4.1	9
F05	3.7	6.3	68	F28	6.9	5.6	-20
F06	10.2	8.3	-18	F29	13.2	8.6	-35
F07	5.2	5.2	-2	F30	10.6	9.6	-9
F08	5.4	5.5	1	F31	8.9	6.6	-26
F09	14.5	9.4	-35	F32	7.0	7.5	6
F10	14.4	9.9	-31	F33	5.1	4.2	-18
F11	3.9	4.3	8	F34	7.9	5.6	-30
F12	5.7	5.5	-4	F35	7.3	8.1	10
F13	15.3	9.3	-39	F36	11.3	9.4	-16
F14	11.2	10.3	-8	F37	7.0	6.7	-5
F15	4.9	6.4	29	F38	7.0	5.3	-25
F16	13.4	8.0	-40	F39	7.6	5.7	-25
F17	3.7	4.2	12	F40	7.2	7.7	7
F18	4.9	5.4	9	F41	6.9	7.9	15
F19	12.7	9.2	-27	F42	6.8	6.1	-10
F20	10.4	10.3	-2	F43	6.8	7.3	7
F21	4.6	5.8	25	F44	3.9	4.0	2
F22	11.8	8.2	-30	F45	5.0	5.3	6
F23	4.8	5.0	5	F46	4.9	7.0	43
–	–	–	–	F47	4.0	8.5	112

Table 8
Supplementary information on settlements

Information	Shell RIG	Shell SSI	Differ. (%)
Maximum settlement (mm)	15.3	10.7	-30
Maximum differential settlement (mm)	12.1	6.7	-44
Average settlement (mm)	7.8	7.0	-10
Coefficient of variation (%)	44	28	-37

settlements after considering the soil-structure interaction. Figures 12 and 13 present the isosettlement curves for the SHELL RIG and SHELL SSI models, respectively. To make the isosettlement curves, the centroid coordinates of each footing were considered in the (x, y) plane and the settlement was adopted as the z coordinate. The linear triangulation interpolation method was used to determine the multiple settlement values of 0.5mm, and thus generate the same value curves.

Observing the isosettlement curves of the SHELL RIG model, it can be observed that the largest settlements are in the region of the S2 borehole, where the soil is more deformable. However, when analysing the soil-structure interaction, a reduction of the settlements in this region can be observed, accounted for by the rigidity of the superstructure that limits differential settlements and redistributes the loads to the neighbouring foundations.

The results show a reduction of 44% in the maximum differential settlement and 30% in the maximum settlement. The reduction in the coefficient of variation emphasizes the tendency of settlement uniformisation caused by the consideration of the soil-structure interaction. The average settlement presented a low reduction, of the order of 10%. When analysing the isosettlement curves, a clear trend of settlement uniformisation can be clearly observed.

5.2 Second series of comparisons

The results of the simplified models are compared and evaluated. In Table 9, the normal (foundation level) stresses of the building walls were compared. Figure 14 shows the diagrams of normal force along the walls studied.

By analysing the results of the normal force on the building´s walls, it can be observed that the simplified models were able to adequately represent the load distribution between the walls. However, there is a perturbation on the second floor. This perturbation is accounted for by the concentration of force at the top of the wall (transition from the column element to the shell element). This characteristic does not interfere in the results, as in all cases the diagram, outside the perturbation region, presented good results, compared to the more refined model.

The MIXED SSI model presented a mean absolute deviation of 9%, where 45% of the walls had excellent results, 44% had good results and only 12% presented results with differences above 18%. The quality of the MIXED SIMP model is somewhat lower, but represents the redistribution of loads between the walls. This model presented a mean absolute deviation of 15%, in which 22% of the results were optimal, 53% good and 25% bad.

Tables 10 and 11 present the comparisons of the loadings on the foundations for the MIXED SSI and MIXED SIMP models, respectively.

The simplified models presented a good approximation of the vertical reactions in the footings, with a mean absolute deviation of 4% and 9% for the MIXED SSI and MIXED SIMP models, respectively. The MIXED SSI model did not present any results outside the acceptable range, with 85% of the results in the optimal range and 15% in the good ones. The MIXED SIMP model presented 38% of the results in the optimal range, 53% in the good and only 9% in the bad one. For the moments applied there is a high divergence between the results.

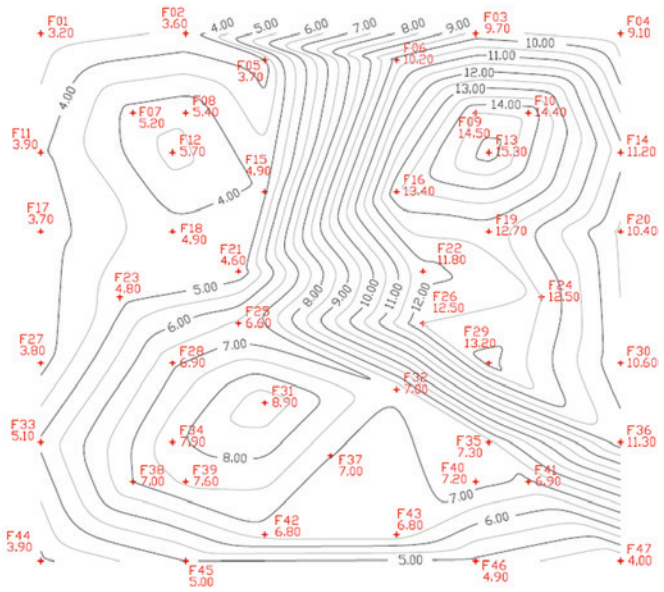

Figure 12
Isosettlement curve of the SHELL RIG model

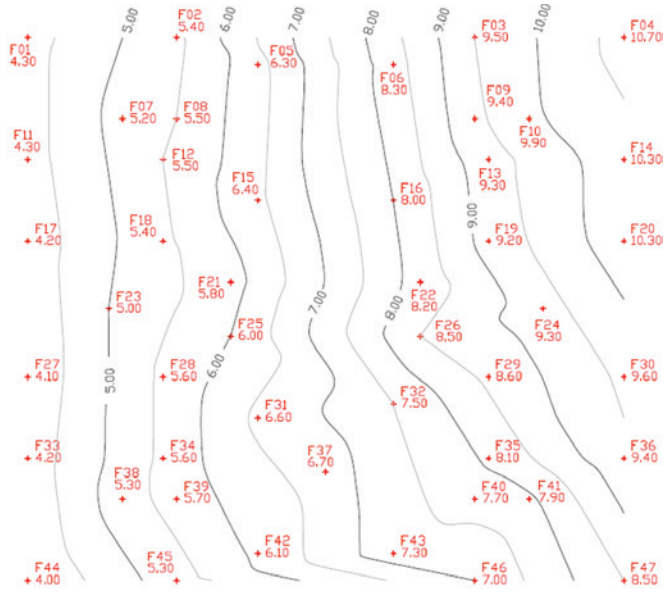

Figure 13
Isosettlement curve of the SHELL SSI model

Table 12 shows the estimated settlements for the building foundations. Table 13 presents some additional information.

The MIXED SSI model presented excellent results, with a difference of 1% in the mean settlement and a difference of 5% for the maximum settlement and maximum differential settlement. In this model, none of the absolute settlements exceeded the 18% difference limit. The MIXED SIMP model presented a mean difference of 2%, 3% for the maximum and the 15% for the maximum differential. In this model only three foundations presented differences higher than the limit of 18%.

6. Conclusions

Consideration of the soil-structure interaction caused a general

Table 9
Normal wall strength in the simplified models – kN

Wall	Shell RIG	Shell SSI	Differ. (%)	Wall	Shell RIG	Shell SSI	Differ. (%)	Shell SSI	Differ. (%)
PH01	265.5	-1	276.1	3	PH45	222.0	14	194.4	0
PH02	28.0	7	27.3	4	PH46	17.3	9	17.8	12
PH03	240.3	-1	329.0	35	PH47	211.7	11	218.2	14
PH04	260.4	-3	180.7	-33	PH48	230.1	-3	254.0	7
PH05	20.0	7	19.4	4	PH49	37.0	4	32.3	-9
PH06	282.0	-1	257.2	-9	PH50	445.2	3	304.2	-29
PH07	60.0	15	46.8	-10	Column	630.0	0	630.0	0
PH08	197.4	-6	185.9	-11	PV01	542.5	10	650.0	32
PH09	45.7	-9	54.5	8	PV02	223.7	15	159.0	-18
PH10	63.0	21	71.5	37	PV03	199.5	2	160.0	-18
PH11	171.9	-2	166.4	-5	PV04	703.1	-2	249.6	-65
PH12	132.4	7	138.2	12	PV05	14.8	20	16.1	31
PH13	362.8	-9	523.0	31	PV06	234.8	3	216.7	-5
PH14	251.4	-2	258.1	0	PV07	6.0	-19	5.0	-33
PH15	509.7	2	501.9	1	PV08	315.2	5	353.3	18
PH16	584.8	-7	810.0	29	PV09	357.0	-4	418.6	13
PH17	477.9	2	500.2	7	PV10	378.7	2	410.2	11
PH18	-26.0	47	-23.0	30	PV11	538.6	-2	537.4	-2
PH19	26.0	44	27.6	53	PV12	473.3	3	414.1	-10
PH20	-9.0	39	-7.0	8	PV13	565.8	-2	530.0	-8
PH21	135.4	5	149.7	16	PV14	569.9	-4	535.8	-10
PH22	214.9	0	214.9	0	PV15	1237.7	9	1327.7	17
PH23	-30.0	-18	-29.0	-21	PV16	1601.4	-5	1531.3	-9
PH24	-73.6	-4	-68.9	-10	PV17	13.5	-1	14.7	8
PH25	214.9	0	214.9	0	PV18	21.0	-2	17.2	-20
PH26	111.0	-14	120.0	-7	PV19	1510.0	14	1440.5	9
PH27	28.4	14	27.8	11	PV20	732.2	-6	823.1	6
PH28	32.4	14	25.8	-10	PV21	449.8	15	470.8	20
PH29	4.0	19	5.0	48	PV22	560.0	-4	568.6	-2
PH30	31.1	10	32.8	16	PV23	368.5	1	358.6	-2
PH31	550.5	-9	887.0	47	PV24	468.9	5	449.6	1
PH32	386.6	-4	438.8	9	PV25	368.3	9	356.5	6
PH33	108.0	2	91.4	-14	PV26	483.4	-4	473.7	-6
PH34	339.4	9	347.9	12	PV27	291.3	7	317.0	17
PH35	303.6	-14	236.0	-33	PV28	3.0	-13	3.0	-13
PH36	233.8	-10	273.3	6	PV29	250.0	14	224.0	2
PH37	145.0	8	145.2	8	PV30	8.4	6	9.4	19
PH38	204.8	-6	198.4	-9	PV31	912.0	-6	1001.7	3
PH39	28.4	2	27.1	-3	PV32	245.1	5	213.1	-9
PH40	90.6	-7	81.4	-17	PV33	256.2	8	207.8	-12
PH41	43.4	29	27.7	-17	PV34	804.0	13	786.7	10
PH42	123.1	-3	124.7	-1	SUM	25059.1	–	25179.1	–
PH43	285.0	-33	289.6	-32	Average	–	9	–	15
PH44	103.0	-33	72.0	-53	–	–	–	–	–

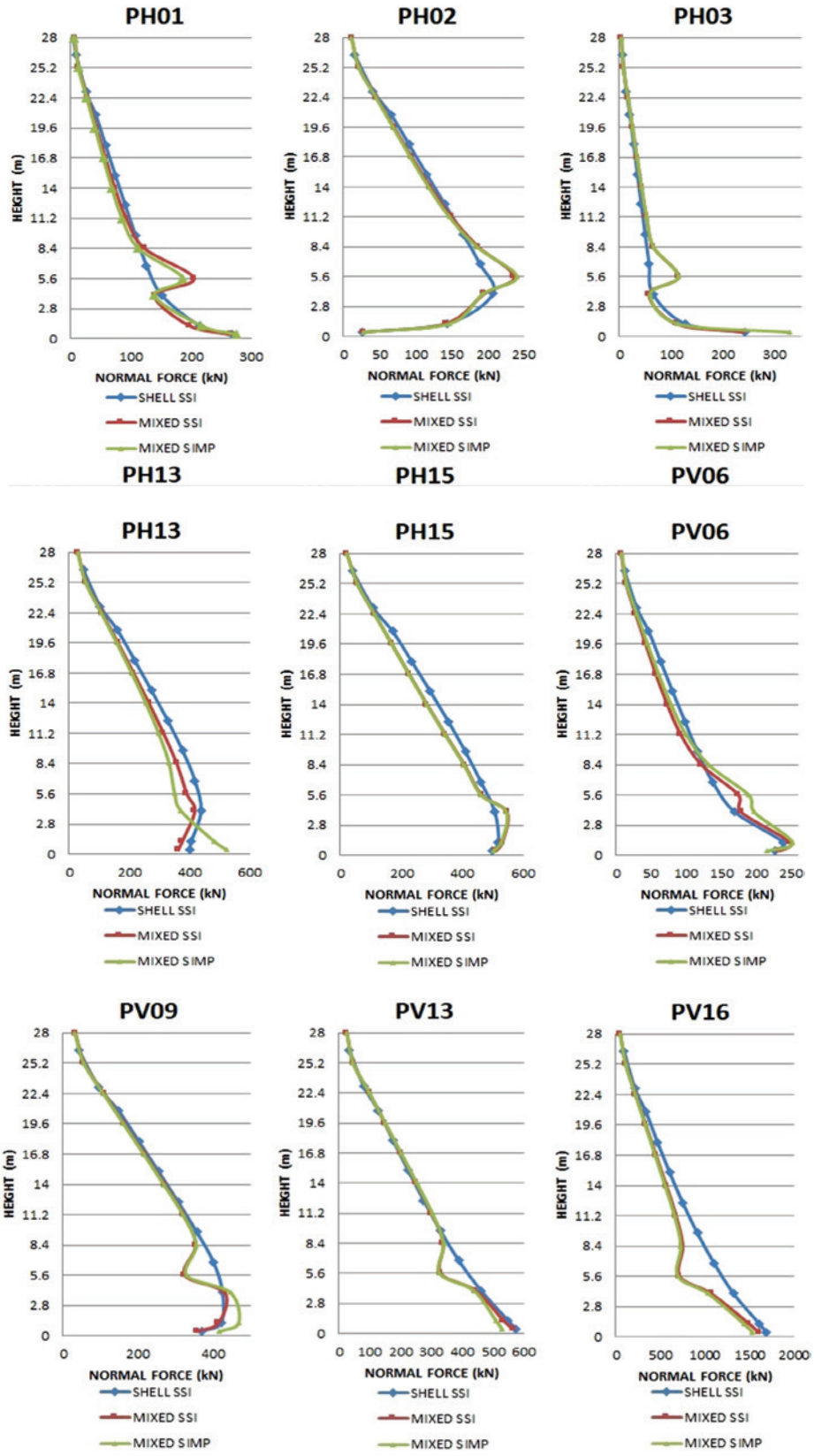

Figure 14
Normal force diagram of the walls of the simplified models

Table 10
Loading on the foundations of the mixed model SSI – kN and kN.m

Found.	Nz		Mx		My	
	Mixed SSI	Differ. (%)	Mixed SSI	Differ. (%)	Mixed SSI	Differ. (%)
F01	682.2	-3	-68.6	2	-84.1	1
F02	768.3	-3	-24.6	-206	2.9	98
F03	570.8	7	0.0	0	-16.0	24
F04	657.2	5	-1.4	-106	-71.0	-1359
F05	1032.6	-4	0.0	0	0.0	0
F06	468.1	0	0.0	0	-9.6	-213
F07	502.1	-3	0.0	0	0.0	0
F08	248.5	-5	0.0	0	0.0	0
F09	190.0	6	0.0	0	0.0	0
F10	399.1	6	0.0	0	0.0	0
F11	771.7	-4	0.0	0	-110.8	-20
F12	273.3	-2	0.0	0	0.0	0
F13	191.2	4	0.0	0	0.0	-100
F14	750.6	4	0.0	0	0.0	0
F15	1164.9	-3	0.0	0	-61.3	11
F16	499.3	-1	0.0	0	8.7	-154
F17	525.1	-4	10.5	-327	-86.8	-18
F18	561.8	-3	42.0	1	0.0	0
F19	410.9	6	16.9	118	-10.9	-37
F20	524.2	5	0.0	0	0.0	0
F21	515.9	-1	-38.8	22	-30.4	-17
F22	272.9	6	0.0	0	0.0	0
F23	645.4	1	0.0	0	-115.1	5
F24	454.8	3	16.5	130	-19.1	-1104
F25	325.2	-1	0.0	-100	-72.9	38
F26	196.0	5	0.0	0	0.0	0
F27	595.2	4	-39.8	-156	-96.7	-15
F28	418.1	3	-11.9	31	0.0	0
F29	253.5	-5	0.0	0	0.0	0
F30	490.6	1	0.0	0	0.0	0
F31	929.9	5	0.0	0	-119.1	7
F32	1175.0	4	0.0	0	47.0	47
F33	610.0	3	0.0	0	-98.6	-47
F34	195.9	1	0.0	0	0.0	0
F35	367.4	-3	0.0	0	10.5	-143
F36	581.7	-1	0.0	0	0.0	0
F37	630.0	0	0.0	0	-136.7	-1
F38	428.6	4	0.0	0	0.0	0
F39	219.5	5	0.0	0	1.2	-136
F40	240.6	-9	0.0	0	2.1	-31
F41	691.9	-4	3.1	-82	0.0	0
F42	771.4	4	0.0	0	0.0	0
F43	904.7	-3	0.0	0	-30.0	-95
F44	548.7	1	49.7	-39	-83.2	12
F45	659.2	3	9.7	-246	0.0	0
F46	733.2	-10	8.1	-208	-25.1	-53
F47	1138.8	-2	112.2	-16	99.9	189
Total	26185.8	–	–	–	–	–
Average	–	4	–	38	–	85

Table 11
Loading on the foundations mixed model SIMP-kN and kN.m

Found.	Nz		Mx		My	
	Mixed SIMP	Differ. (%)	Mixed SIMP	Differ. (%)	Mixed SIMP	Differ. (%)
F01	708.7	1	-83.4	24	-91.7	10
F02	747.1	-6	199.7	763	41.6	2747
F03	547.7	2	0.0	0	-25.5	98
F04	655.8	4	-61.9	-391	20.8	268
F05	963.4	-10	0.0	0	0.0	0
F06	483.3	3	0.0	0	29.9	252
F07	563.5	9	0.0	0	0.0	0
F08	288.4	10	0.0	0	0.0	0
F09	198.6	11	0.0	0	0.0	0
F10	432.9	15	0.0	0	0.0	0
F11	895.7	11	0.0	0	-704.0	407
F12	302.5	9	0.0	0	0.0	0
F13	204.9	11	0.0	0	-17.2	1565
F14	747.6	4	0.0	0	0.0	0
F15	1132.0	-5	0.0	0	-62.3	13
F16	541.2	7	0.0	0	-5.2	-67
F17	393.9	-28	-194.0	4085	-689.3	550
F18	561.0	-3	36.9	-11	0.0	0
F19	389.3	0	20.4	162	-13.1	-23
F20	499.6	0	0.0	0	0.0	0
F21	453.0	-13	-49.1	54	-31.7	-13
F22	255.8	0	0.0	0	0.0	0
F23	631.5	-1	0.0	0	-160.6	46
F24	461.8	5	-1.0	-114	30.3	1493
F25	357.1	9	10.3	882	-69.2	31
F26	245.5	31	7.9	0	0.0	0
F27	529.5	-7	416.7	489	-327.3	188
F28	438.6	8	-32.5	257	0.0	0
F29	338.8	27	0.0	0	0.0	0
F30	462.3	-5	0.0	0	0.0	0
F31	1055.3	19	0.0	0	-90.5	-19
F32	1022.4	-10	0.0	0	37.8	18
F33	628.9	6	0.0	0	247.5	-233
F34	223.0	15	0.0	0	0.0	0
F35	334.5	-11	0.0	0	-22.4	-9
F36	631.6	8	0.0	0	0.0	0
F37	630.0	0	0.0	0	-8.6	-94
F38	463.9	13	0.0	0	0.0	0
F39	235.7	12	0.0	0	12.1	-457
F40	297.5	12	0.0	0	26.2	777
F41	689.6	-4	4.5	-74	0.0	0
F42	755.5	2	0.0	0	0.0	0
F43	916.6	-2	0.0	0	-83.4	-85
F44	544.6	0	97.6	21	-114.5	54
F45	585.5	-8	-61.0	823	0.0	0
F46	699.4	-14	-79.0	956	-46.8	-13
F47	1040.7	-10	263.5	97	35.0	1
Total	26185.8	–	–	–	–	–
Average	–	9	–	196	–	203

Table 12
Settlement for simplified models – mm

Found.	Mixed SSI	Differ. (%)	Mixed SIMP	Differ. (%)	Found.	Mixed SSI	Differ. (%)	Mixed SIMP	Differ. (%)
F01	4.2	-2	3.4	-21	F24	9.5	2	9.6	3
F02	5.1	-4	5.1	-5	F25	5.9	-1	6.1	2
F03	10.2	7	9.9	4	F26	8.7	2	9.5	12
F04	11.2	4	11.1	3	F27	4.3	5	3.6	-11
F05	6.0	-4	5.8	-9	F28	5.6	1	5.7	3
F06	8.3	0	8.5	2	F29	8.7	1	9.8	14
F07	5.0	-3	5.4	5	F30	9.9	4	9.4	-2
F08	5.3	-3	5.9	7	F31	6.7	1	7.4	11
F09	10.0	6	10.5	12	F32	7.6	2	7.2	-4
F10	10.5	7	11.1	12	F33	4.3	3	4.7	11
F11	4.2	-2	5.7	33	F34	5.6	0	6.2	11
F12	5.3	-3	5.8	5	F35	8.2	2	7.7	-5
F13	9.8	6	10.4	12	F36	9.4	-1	9.7	3
F14	10.9	6	10.8	5	F37	6.4	-4	6.8	2
F15	6.2	-3	6.0	-5	F38	5.3	1	5.8	10
F16	7.9	-1	8.5	6	F39	5.8	2	6.3	10
F17	4.1	-2	3.4	-19	F40	7.8	1	7.7	0
F18	5.2	-3	5.1	-6	F41	8.2	3	7.8	-1
F19	9.3	1	9.2	0	F42	6.0	-2	6.3	3
F20	10.6	4	10.1	-1	F43	7.0	-4	7.3	0
F21	5.7	-2	5.3	-8	F44	4.2	4	4.1	4
F22	8.5	3	8.5	4	F45	5.4	2	5.2	-3
F23	5.0	0	4.2	-17	F46	7.5	7	6.3	-10
–	–	–	–	–	F47	8.2	-4	7.5	-12

trend towards the standardization of settlements. The maximum differential settlement and the maximum absolute settlement showed a marked reduction. The mean settlement, however, was not very influenced.

The soil-structure interaction provided a redistribution of the loads in the foundations and a significant reduction of the applied moments. As a general rule, there was a load transfer from foundations with higher settlements to the neighbouring foundations of lower settlements.

There were important changes in the normal stresses of the walls. The greatest influence of the soil-structure interaction occurred on the first floors, where there were differences greater than 18%, adopted as an acceptable limit in this work.

The simplified models adequately represented the stress flow on the walls and the load distribution on the foundations. The MIXED SSI model presented the best results.

Table 13
Supplementary information on simplified model settlements

Information	Mixed SSI	Differ. (%)	Mixed SIMP	Differ. (%)
Maximum settlement (mm)	11.2	4	11.1	3
Maximum differential settlement (mm)	7.1	5	7.7	15
Average settlement (mm)	7.1	1	7.2	2
Coefficient of variation (%)	30	7	31	9

7. Acknowledgments

The authors gratefully acknowledge CNPq (National Council for Scientific and Technological Development) for the financial support.

8. References

[1] NUNES, V. Q. G. Análise estruturais de edifícios de paredes de concreto armado, São Paulo, 2011, DSSIertação (Mestrado) - Escola de Engenhari de São Carlos, Universidade de São Paulo (in Portuguese).

[2] BRAGUIM, T. C. Utilização de modelos de cálculo para projetos de edifícios de paredes de concreto armado moldadas no local, São Paulo, 2013, DSSIertação (Mestrado) - Escola Politécnica, Universidade de São Paulo (in Portuguese).

[3] ASSOCIAÇÃO BRASILEIRA DE NORMAS TÉCNICAS. Paredes de concreto moldadas no local para construção de edificações. - NBR 16055, Rio de Janeiro, 2012 (in Portuguese).

[4] MEYERHOF, G. G. Some recent foundation research and its application to design. Structural Engineering, v.31, n.2, 1953; p.151-167.

[5] CHAMECKI, S. Structural rigidity in calculating settlements. Journal of Soil Mechanics and Foundation Division, v.82, n.SM-1, 1956; p.1-19.

[6] GOSHY, A. D. Soil-foundation-structure interaction. Journal of Structural the Division, v.104, 1978; p.749-761.

[7] GUSMÃO, A. D. Aspectos relevantes da interação solo-estrutura em edificações. Solos e Rochas, v.17, 1994; p.47-55 (in Portuguese).
[8] TESTONI, E. Análise estrutural de edifícios de paredes de concreto por meio de pórtico tridimensional sobre apoios elásticos, São Paulo, 2013, DSSIertação (Mestrado) – Escola de Engenharia de São Carlos, Universidade de São Paulo (in Portuguese).
[9] TESTONE, E. Análise de interação solo-estrutura em edifícios de paredes de concreto moldadas no local. Revista Fundações e Obras Geotécnica, v.6, 2016; p.36-46 (in Portuguese).
[10] SANTOS, M. G C. Análise estrutural dos efeitos dos deslocamentos dos apoios de edifícios de paredes de concreto moldadas no local, São Paulo, 2016, DSSIertação (Mestrado) – Escola de Engenharia de São Carlos, Universidade de São Paulo (in Portuguese).
[11] LIU, Y. P. *et al*. Second-order Analysis and design of wall-framed structures allowing for imperfections. Advances in Structural Engineering, v.13, n.3, 2010; p.513-524.
[12] YAGUI, T. Estruturas constituídas de paredes delgadas com diafragmas transversais, São Paulo, 1971, Tese (Doutorado) – Escola de Engenharia de São Carlos, Universidade de São Paulo (in Portuguese).
[13] YAGUI, T. Análise de estruturas de edifícios construídas de núcleos de concreto armado e pilares ou pendurais de aço (carregamento crítico de instabilidade), São Paulo, 1978, Tese (livre-docência), Universidade de Campinas (in Portuguese).
[14] CORRÊA, M. R. S. Aperfeiçoamento de modelos usualmente empregados no projeto de sistemas estruturais de edifícios, São Paulo, 1991, Tese (Doutorado) – Escola de Engenharia de São Carlos, Universidade de São Paulo (in Portuguese).
[15] NASCIMENTO NETO, J. A. Investigação das solicitações de cisalhamento em edifícios de alvenaria estrutural submetidos a ações horizontais, São Paulo, 1999, DSSIertação (Mestrado) – Escola de Engenharia de São Carlos, Universidade de São Paulo (in Portuguese).
[16] AOKI, N. Aspectos geotécnicos da interação estrutura-maciço de solos. *In*: XXVIII Jornadas Sul-Americanas de Engenharia Estrutural, São Carlos, 1997, Anais, São Carlos, 1997 (in Portuguese).
[17] MINDLIN, R. D. Force at a point in the interior of a semi-infinite solid. Physics, v.7, 1936; p.195-202.
[18] STEINBRENNER, W. Tafeln zur setzungsberechnung. Die Strasse, v.1, 1934; p.121.
[19] REIS, J. H. C. Interação solo-estrutura de grupo de edifícios com fundações superficiais em argila mole, São Paulo, 2000, DSSIertação (Mestrado) – Escola de Engenharia de São Carlos, Universidade de São Paulo (in Portuguese).
[20] ASSOCIAÇÃO BRASILEIRA DE NORMAS TÉCNICAS. Cargas para o cálculo de edificações. - NBR 6120, Rio de Janeiro, 1980 (in Portuguese).
[21] ASSOCIAÇÃO BRASILEIRA DE NORMAS TÉCNICAS. Ações e segurança nas estruturas - procedimento. - NBR 8681, Rio de Janeiro, 2003 (in Portuguese).